

An Equivalent Circuit Planar Magnetics Inductors Model vs air gap and Parameter Extraction Based on the Genetic Algorithm

Aymen Ammouri^{#1}, Tarek Ben Salah^{#1,2}, Ferid Kourda^{#1}

^{#1} Université de Tunis El Manar, ENIT-L.S.E, BP 37-1002, Tunis le Belvédère, Tunis, Tunisie

^{#2} Technical and Vocational Training Corporation, College Of Technology in Tabuk, KSA

Abstract-- The adjustment for the required inductance is quite straightforward by controlling the air gap of the magnetic core. The focal point basis is the dependence on air gap and the windings effects. An advanced magnetics planar inductor model is developed. The magnetic inductor remains a difficult device to model mainly, particularly when air gap are taken into account. A novel physically based analytical model is used to accurately simulate this planar magnetic inductor. The skin and proximity effects in metal lines of planar inductor are represented as the impedance of a ladder R-L networks. These R-L ladder parameters are determined by minimizing the errors function between experimental and simulation results using the genetic algorithm. During validation process, different type of magnetic core has been investigated. The planar inductor model results have been favorably evaluated by comparison and validation with practical measurements and to 3D finite element method simulations. It is found that simulation results and measurements data are in close agreement of the inductive and the parasitic effects.

Index Terms-- Planar Inductor Model, finite element methods (FEM), R-L Ladder network, Genetic Algorithm.

1. INTRODUCTION

The large mass/volume of a given power converter system is occupied by the magnetic components [1, 2]. A continuous miniaturization of power converter integrating planar magnetics is leading to low profile, higher performance, higher efficiency, decreasing costs and higher thermal characteristics [3-5]. Moreover, planar technology cores have a higher surface area to volume ratio compared with conventional magnetic cores, therefore planar components having lower thermal resistance and consequently cores losses [2].

These magnetic components may be optimized using planar PCB devices. Compared to the conventional magnetic components, planar technology is printed directly on circuit board (PCB) with low profile and offers the flexibility of winding geometry [3, 4].

From a design point of view, accurate planar magnetic inductors models are necessary to design an integrated power converter [5, 6]. In particular, the skin and the proximity effects, the parasitic capacitances effects, the eddy current effects and the air gap in the magnetic core are complex devices to model, particularly during high frequency application [7]. In [8], the finite element method (FEM) is considered to modeling magnetic components. However, this method is not only difficult to develop into general electronically circuit simulations and it is time consumption and not only cumbersome. In [9] an empirical magnetic inductor model is presented.

Although, this model is declared accurate, this model is not depended on the geometrical parameters and the layout design. Moreover, its model parameters are not used fairness to optimize the planar inductor layout.

In this paper, a novel magnetic planar inductor model with air gap is proposed. This model is then taken into account the skin and proximity effects in the metal lines and the parasitic capacitances effects between layers. Therefore a more advanced model is then considered to take into account the variation of the resistance of planar inductor according to the frequency. Then, a ladder R-L network has been used to take into account the skin and proximity effects in the metal lines.

Moreover, the proposed model includes the effects of air gaps in the magnetic core necessary to control the inductance value. Based on the work developed in [3,7], planar inductors integrated in power converters are fabricated with air gaps. The presence of an air gap is the inductors is necessary to linearize the behavior of an planar inductor over a large excursion range of the winding current, avoiding core saturation and reducing the harmonic distortion [3,7]. It is also important to note, magnetic planar inductor can be adjusted by controlling the air gap without modifying the dimensions of the magnetic materials or copper windings. On the other hand, when the planar inductors are used with air gap, we can suppress the temperature dependency into the magnetic core. Thus, for the planar inductor with air gap, we can improve performance such as a high quality factor and maintain higher values of inductance. Therefore, planar inductor with air gap is a key point for designing efficient power converter, requiring then accurate model.

The principal purpose of this paper is to present an accurate planar inductor model with air gap. After the development of the planar inductors model, a step-by-step process is proposed to validate the gapped planar inductors.

- Step#1 dwells on the analysis of distributed-gap in the planar inductors.

- Step#2 illustrates the test and the validation process by comparing the proposed model with the experimental measurements and with the 3D FEM simulation. The errors between analytical and simulation results are computed. First, the errors between experimental and simulation results of the inductive effect are computed and plotted on histograms to estimate the validation quality. Second, a comparative study between experiment and simulation results at frequency domain for series resistance is established. Finally, the parasitic capacitance model is validated with FEM 3D.

2. MODEL DESCRIPTION

Figure 1a shows the proposed magnetic planar inductor printed on FR4-PCB substrate. This device is designed by two main elements: the planar windings printed on PCB substrate and the planar magnetic circuit used for channeling the magnetic field line. The planar winding geometric parameters are; w is the width of the trace, t is the thickness of the metal trace, S is the spacing between turns, n_l is the number of turns per layer and N_l is the number of layers. Figure 1b illustrates the equivalent circuit model of a magnetic planar inductor [4, 6]. This model includes the total inductance L_s , the parasitic capacitance C_s between layers and the skin and proximity effects in metal trace are modeled by an RL ladder network [9]. The ladder R-L network is mainly depended to the current crowding in the metal. The total inductance L_s is the sum of the main inductance including the corner effect and the winding inductance.

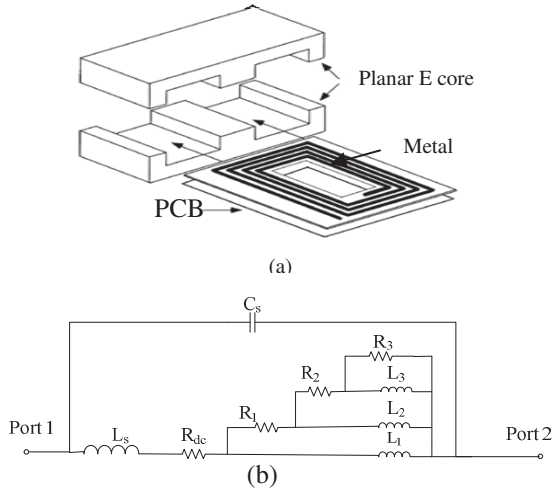


Fig. 1. The proposed planar inductor: (a) picture and (b) equivalent circuit model.

A. Planar Inductance without air gap model

Based in [8], an improved model to calculate the total self inductance of a planar inductor with magnetic core is developed. This inductance model can be computed by summing the magnetic core inductance and the winding of copper tracks. Therefore, the total dc inductance of magnetic planar inductors is expressed by equation (1):

$$L_s = L_{core} + L_{winding} \quad (1)$$

Where L_{core} is the inductance of the core and $L_{winding}$ is the inductance of the planar winding inductor.

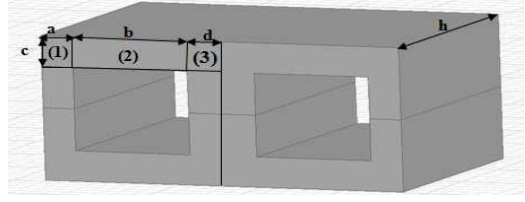
Generally, the inductance contribution from the magnetic core can be estimated by equation (2).

$$L_{core} = \mu_0 \mu_r \frac{A_e}{l_e} N^2 \quad (2)$$

Where N is the number of turns in winding, A_e is the core cross-section area and l_e the equivalent length of magnetic path. The parameters μ_0 and μ_r are the permeability vacuum and the relative permeability of the core material, respectively. It is important to note that, in the magnetic core, the flux tends to concentrate on the inside the bend

(corner), so decrease the mean magnetic path [7]. This model takes into account the corner in the magnetic core. Based on this textbook, a sample model to calculate the parameters of corner are developed in [3, 7]. This model can be computed by summing the self inductance of all cross-sections included the cross-section of the corner. The cross-section and magnetic path length calculation of the straight sections is quite simple whereas compared to the corner sections is more complicated. The mean magnetic path length and cross-section of each corner segment is illustrated in Table I.

Table I. Magnetic path length and cross-section for the planar core calculation.



| | Section (1) | Section (2) | Section (3) |
|--|-------------------|-------------|-------------------|
| Cross-section area (A_c) | $h.(a + c)/2$ | $h.c$ | $h.(d + c)/2$ |
| Equivalent length of magnetic path (l_e) | $(\pi/8).(a + c)$ | b | $(\pi/8).(d + c)$ |

Therefore, the reluctance of an each rectangular cross-section area can be calculated by:

$$R_{c,i} = \frac{l_i}{\mu_0 \mu_r A_i} \quad (3)$$

Where A_i is the core cross-section area and l_i is the equivalent length of magnetic path.

The total core inductance of the inductor is expressed by equation (4):

$$L = \frac{N^2}{R_{c,tot}} \quad (4)$$

Where N is the number of turns of the winding and $R_{c,tot}$ is the total reluctance of magnetic core.

The total inductance $L_{winding}$ of the spiral inductor is obtained by equation (5):

$$L_{winding} = \sum_i^{N_L} L_{win,i} + 2M_{Multilayer} \quad (5)$$

Where $L_{win,i}$ is the self inductance of planar inductor in each layer, M_{ij} is the mutual inductance between two planar inductors and N_L is the number of layers.

More other details of multilayer planar inductor model are illustrated in [4, 10].

B. Planar Inductance with Air gap model

Different methods have been proposed in the literature to model the air gap in inductor [7]. The major calculations of the air gap reluctance for the planar inductor are based on two magnetic core type. The cores are a pair of EE and EI 43/10/28-3F3 planar core from Ferrocube. Three types of air gap cross sections which are illustrated in Figure 2. The basic air gap reluctance model is expressed by equation (6).

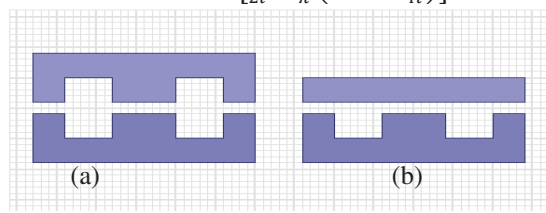
$$R_{basic} \cong \frac{1}{\mu_0 \left[\frac{w}{2l} + \frac{2}{\pi} \left(1 + \ln \frac{\pi h}{4l} \right) \right]} \quad (6)$$


Fig. 2. Planar magnetic core: (a) EE core (b) EI core.

The equivalent magnetic circuit models of air gap reluctance calculation are illustrated in Figure 3. To obtain a reluctance associated with the air gap with a good accuracy, it is essential to consider 3D phenomena, i.e. taking into account the swelling of the field lines. To consider the swelling of the field lines of 3D air gaps, [7] proposes an improved model to calculate the 3D air gap reluctance of a transformer. In this model a fringing factor is introduced that describes by which factor the air gap reluctance decreases due to fringing flux. The reluctance of the 3D air gap can be expressed by equation (7) [7]:

$$R_{air\ gap,i} = \sigma_x \sigma_y \frac{a}{\mu_0 t b} \quad (7)$$

Where

$$\sigma_x = \frac{R_{basic}}{a / \mu_0 t} \quad (8)$$

$$\sigma_y = \frac{R_{basic}}{a / \mu_0 b} \quad (9)$$

Where a , b and t are the geometrical parameters for the two type's planar magnetic core with air gap (Figure 3). The parameters σ_x and σ_y are the fringing factor that considers fringing effects in y -direction and x -direction, respectively. More other details for the air gap reluctance model calculation and are given in [7].

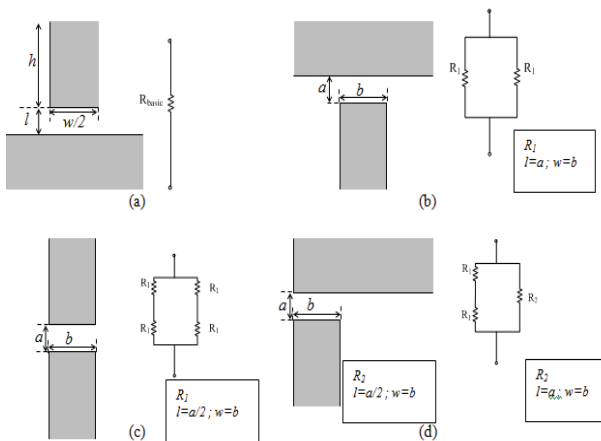


Fig. 3. Different types of air gaps and equivalent circuit reluctance models: (a) Basic geometry of air gap (b) Air gap type#1 (c) Air gap type#2 and (d) Air gap type#3.

C. Winding loss model

Ferreira [11] proposes a model to calculate the AC resistance of planar magnetic components. Based on [11],

planar inductor model and its associated parameters are detailed in a previous work [12, 13]. But, from a design point of view, a limitation of the current model versus frequency is verified and does not give satisfactory results. Thus, the planar inductor behaviour cannot be precisely predicted by the conventional inductor models [12]. In [12, 13], the error between the FEM 3D simulation and the analytical model results of planar inductor model is around than 25%. The error observed in the series resistance can be explained by many problems. Firstly, the problem is one-dimensional (H only depends on a dimension) and the density distribution of the currents in the conductors is uniform. Secondly, the corners present in the planar topologies, do not promote a homogeneous distribution of current in the conductor at these corners. Indeed, it is very likely that the current lines accumulate inside of the angle, increasing the current density is inside relative to the outside, which results in an increase resistance of the coils. However, the planar inductor remains a difficult component to model, particularly when the influence of skin and proximity effects is taken into account. There are various methods available to model the skin and proximity effects in the planar inductor [2-4]. In the present study, an R-L ladder circuit was used to model the evolution of the resistance with the frequency as shown in figure 1b. A ladder R-L network is built with resistors and inductors to take into account variations of the resistance with frequency. The values of this R-L circuit network were determined by a genetic algorithm from the measuring points of the evolution of the resistance versus frequency for a planar inductor [14,15]. To determine the ladder R-L equivalent circuit model of planar inductor resistance, a methodology based on the genetic algorithm (GA) is proposed.

D. Parasitic capacitance model

The parasitic capacitances between turns and between winding layers are creating by the distribution of the voltage potential. The turns to turns capacitance can be neglected due to the dominating inter-layers winding capacitance. The parasitic capacitance between two layers in winding is modeled using the parallel-plate capacitance. Where the planar inductor winding consists of m uniform layers connected in series, the equivalent capacitance can be calculated by equation (10) [16]:

$$C_s = \frac{4(m-1)}{3} \frac{C_l}{m^2} \quad (10)$$

$$C_l = \left(\frac{(n+1)(2n+1)}{6n} \right) C_0 \quad (11)$$

$$C_0 = \epsilon_0 \epsilon_r \frac{\omega * l}{H} \quad (12)$$

Where n is the number of turns in each layer and C_0 is the equivalent parallel plate capacitance of a two adjacent layers. ϵ_0 is the permittivity of air space, ϵ_r is the relative permittivity of dielectric material, 4.4 for FR-4. ω is the width of the trace, l is the average length of a turn and H is the distance between two parallel plate.

3. STEP-BY-STEP VALIDATION PROCESS

Step #1: Planar inductor parameter optimization

During optimization process, low winding loss planar inductors factor are studied by analyzing the effect of different formats of air gaps for given device [17]. Figure 4 shows a comparative study between three planar inductors with different air gap distributed. These results present the AC resistance of planar inductors. It is worth mentioning that, the air gap length parameter to the three Sample#1, Sample#2 and Sample#3 are 0.3, 0.3 and 0.1 mm, respectively. Reveals that the low ac winding is obtained where air gap distributed in all legs of magnetic core. For that reason, we are interested in the structures of planar inductors where the air gaps are distributed in the centre and laterals legs (Sample#3 in figure 4). Based on the developed model introduced in previous section, several planar inductors are designed, simulated, and built using PCB-FR4 as a substrate. Designed planar inductors are simulated using Ansoft Maxwell 3D, fabricated and measured using LCR meter Analyzer.

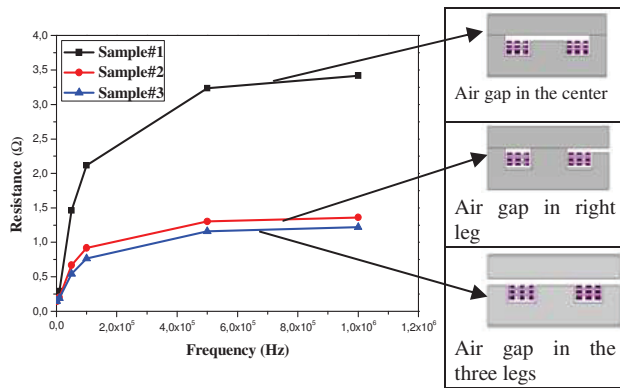


Fig. 4. AC winding resistance versus different format of air gap.

Different planar inductors designs are used during simulation and experimental process. The core is a pair of EE and EI 43/10/28–3F3 planar core from Ferroxcube. These planar inductors are designed by a multilayer PCB made on FR-4 material with the copper thickness, the dielectric constant, ϵ_r , and the PCB substrate thickness are 35 μm 4.4 and 1.6 mm, respectively. Design parameters of the planar inductors are depicted in Table II.

Step#2: Validations and Discussion

A. Planar inductor without air gap

To validate the proposed planar inductor model, two types of magnetic circuit (the standard planar ferrite EE and EI core) are used. Different magnetic planar inductors with air gaps designs are tested during experimental steps. The lumped air gaps are distributed between central and outer core legs. Design parameters of the planar inductors are depicted in Tables II. In order to validate air gap planar inductor model, the air gap length is also tuned from 0.13 toward 0.4 mm. The planar inductors with EE and EI-43/10/28–3F3 Ferroxcube ferrite core are tested using LCR meter. A validation procedure is performed by a comparative study between simulation results with finite

element model as well as with experimental results for planar inductors devices. Tables III depict a comparative study between experimental data, 3D FEM simulation and new and conventional analytical model of the inductive effect.

Table II. Geometrical parameters of planar inductor used during simulation steps.

| Geometrical Parameters | EE planar core 43/10/28–3F3 | | | | EI planar core 43/10/28–3F3 | |
|------------------------|-----------------------------|----------|----------|----------|-----------------------------|----------|
| | Sample#1 | Sample#2 | Sample#3 | Sample#4 | Sample#5 | Sample#6 |
| w (mm) | 3 | 2.2 | 3 | 2.2 | 3 | 2.2 |
| s (mm) | 0.8 | 0.5 | 0.8 | 0.5 | 0.8 | 0.5 |
| n_t | 3 | 4 | 3 | 4 | 3 | 4 |
| N_{i_layer} | 6 | 6 | 7 | 7 | 4 | 4 |
| N | 18 | 24 | 21 | 28 | 12 | 16 |

An error function named δ is computed. This function is computed from the following expression [4]:

$$\gamma = \left| \frac{f_{EXP}(x_i) - f_{SIM}(x_i)}{f_{EXP}(x_i)} \right| \quad (13)$$

Where f_{EXP} and f_{SIM} are the electrical quantities extracted from the experimental data and analytical model, respectively.

Table III. Analytical results for spiral inductors.

| | | Measurement | 3D FEM Simulation (μH) | New analytical method Calculation (μH) | Classically Calculation (μH) |
|----------------|----------|-------------|-------------------------------------|---|---|
| EE planar core | Sample#1 | 2475.6 | 2499.6 | 2553.5 | 2252.2 |
| | Sample#2 | 4487.3 | 4444.3 | 4539.8 | 4004.5 |
| | Sample#3 | 3440.5 | 3400.2 | 3475.2 | 3065.5 |
| | Sample#4 | 6086.1 | 6044.7 | 6180.7 | 5449.9 |
| EI planar core | Sample#5 | 1407 | 1382 | 1410.6 | 1202.7 |
| | Sample#6 | 2445.5 | 2467.5 | 2507.9 | 2138.1 |

The validity histogram of the proposed inductive model depicts in Figure 5 is obtained by a comparative study between simulation results and experimental data for many planar inductors devices. The error of this model is less than 2% between experimental and simulation results compared with 15% for conventional model (equation 1). On the other hand, the error of this model is less than 2% between FEM simulation and our proposed model. This result is justified by the approximation made to take into account the effects of corner in the magnetic circuits. Indeed, in a rectangular magnetic circuit, the field lines are uniformly distributed in the straight legs, but in the corners, they are moved to the inside of the corner. The flux is denser in an inner area than in the linear portion of the circuit. This difference is due, probably, to his result confirmed that the projected model is more accurate in terms of inductive effect of planar inductor.

For the series resistance of the magnetic planar inductor, the validity of the ladder R-L network model is obtained by a comparative study between simulation results and experimental data for many magnetic devices. Therefore, during identification process, the parameters of ladder R-L network are determined by using Generic Algorithm (GA) toolbox of the MATLAB.

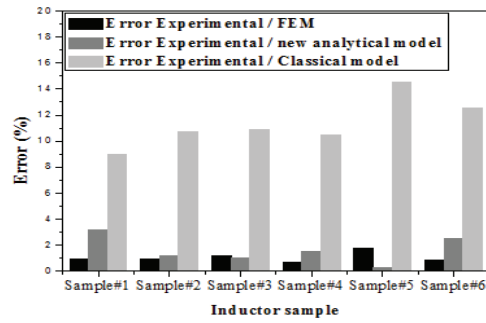


Fig. 5. Errors between experimental and simulations results of inductive effect in planar inductors.

During this phase, the ladder R-L network circuit shown in Figure 1b is used to model the planar inductor windings, which can be decomposed into resistances and inductances. The proposed ladder R-L circuit model is used take into account the evolution skin and proximity effects with the frequency. The proposed method is based on the measurement approach. In a previous study and a physically based compact planar inductor model is developed in [12, 13]. The computed error between the based physical resistance model and the 3D FEM simulation results is about 25%.

Figure 6 shows a comparative study between experimental and simulation results for different planar inductors. These results show good correlation between measured and the proposed model over all the frequency range. Therefore, for the variation of the resistance as a function of frequency, the error between measurement and simulation is negligible over the entire frequency band and are used to validate the model of the planar inductor in the frequency domain.

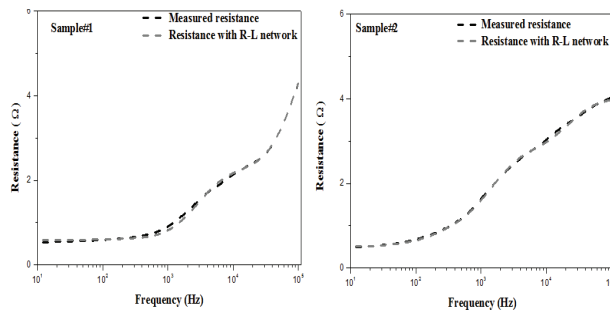


Fig. 6. Comparison between the measured and simulated resistance of the planar inductor model.

The device under test (DUT) is represented with inductance and ladder RL network series connected. On the other hand, to taken into account high frequency effect, an additional element is added in parallel and that correspond to the parasitic capacitance effect introduced by dielectric material. To validate the proposed parasitic capacitance model, different planar inductors tests are considered. Therefore, a comparative study between analytical model and 3D FEM simulation, for many magnetic planar inductors devices is shown in Table IV. Therefore, the obtained results show a good accuracy of the capacitance model.

Table IV. Parasitic capacitance Error between 3D FEM simulation results and analytical model.

| | | 3D FEM simulation C_p (pF) | Analytical model C_p (pF) |
|----------------|----------|------------------------------|-----------------------------|
| EE planar core | Sample#1 | 8.7 | 10 |
| | Sample#2 | 8.7 | 12.1 |
| | Sample#3 | 7.16 | 8.9 |
| | Sample#4 | 7.16 | 10.6 |
| EI planar core | Sample#5 | 14.4 | 13.6 |
| | Sample#6 | 14.4 | 16.3 |

B. Planar inductor with air gap model validation

To improve the accuracy of the analytical model and model the evolution of the magnetizing inductance as a function of variations in the air gap, it is essential to consider the swelling phenomena field lines. Usually, the swelling phenomena of the field lines are not taken into account when calculating the reluctances in conventional manner.

To validate the proposed planar inductor model, two types of magnetic circuit (the standard planar ferrite EE and EI core) are used to fabricate planar inductors. Different magnetic planar inductors with air gaps designs are tested during experimental steps. The lumped air gaps are distributed between central and outer core legs. Design parameters of the planar inductors are depicted in Table II. In order to validate air gap planar inductor model, the air gap length is also tuned from 0.13 toward 0.4 mm. The planar inductors with EE and EI-43/10/28-3F3 Ferroxcube ferrite core are tested using LCR meter.

The validity histograms depicted in figure 7 demonstrate that the error between measured, simulation and analytical model for gapped planar inductors. The error between experimental data and proposed gapped planar inductor model is less than 6% compared with 30% for classical calculation of inductive effect for different air gap length.

On the other hand, where air gap length increase from 0.13 mm to 0.4 mm, the classical method errors increases from 15% to 30%, respectively. Compared to the proposed model the errors are nearly constant with air gap increase.

Therefore, at different air gap length, proposed model and experimental results of the have satisfactory compatibility in terms of inductive effect. This result is justified by the take into account the effects of corner and the swelling of the magnetic field lines in the magnetic circuits [3, 7]. Indeed, the presence of the corner in the magnetic circuit will change consistently the course of the field lines. First, in a rectangular magnetic circuit, the field lines are uniformly distributed in the straight legs, but in the corners, they are moved to the inside of the corner. The second major phenomenon is swelling of the field lines at the air gaps. When adding a gap in magnetic circuit, the fields lines are no longer parallel as in the magnetic material but tend to move away from each other. The field lines occupy a larger area in the air gap in the magnetic circuit.

In addition, proposed gapped planar inductors model can save time during design of the planar magnetic components. Moreover, the analytical model can guide the

geometrical construction of planar magnetic components and also provide a better understanding of the physical phenomena involved through an advanced study.

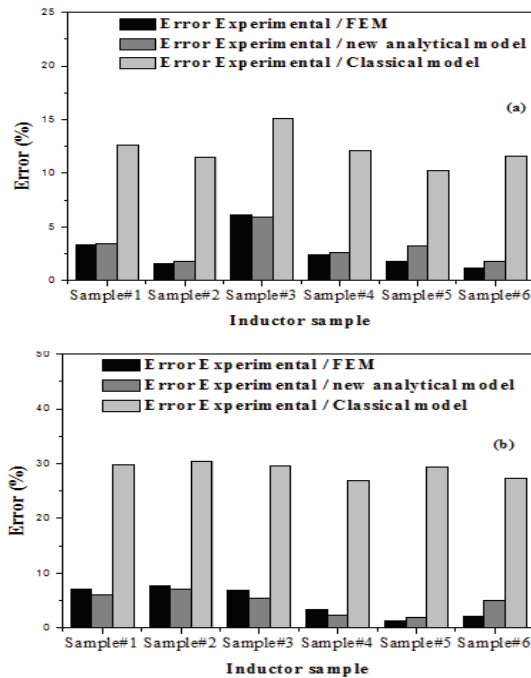


Fig. 7. Error between measured, simulation and analytical results for different planar inductors (a) air gap $g = 0.13\text{mm}$, (b) $g = 0.4\text{mm}$.

4. CONCLUSION

In this paper, an equivalent circuit modelling of magnetic planar inductors has been investigated. Depending on the material and the shape of the core, new planar inductor with air gap model was developed and validated by experimental and 3D FEM computations. The gapped magnetic component model is taking into account the effects of corner and the swelling of the magnetic field lines in the magnetic circuits. Second, the proposed model includes the eddy current effect in the conductor and the parasitic capacitance effects. Therefore, ladder R-L network has been introduced for taking into account the copper losses effects of the planar inductor. The extraction ladder R-L parameters procedure is based on generic algorithm and it leads to very accurate simulation. On the other hand, the parasitic capacitance between the adjacent turns and between adjacent layers is introduced in our model. Large planar inductors samples are designed, manufactured, modeled and experimentally tested. The proposed model is not only dedicated for gapped planar inductor but can be used for any magnetic component such planar transformer.

ACKNOWLEDGMENT

This work was supported by the Tunisian Ministry of High Education and Research under Grant LSE-ENIT LR 11ES15.

References

[1] S. Kimura, Y. Itoh, W. Martinez, M. Yamamoto, J. Imaoka,

Downsizing Effects of Integrated Magnetic Components in High Power Density DC-DC Converters for EV and HEV Applications," IEEE Transactions on Industry Applications, vol. xx, no. 99, (2016).

[2] Ziwei Ouyang, and Michael A. E. Andersen, "Overview of Planar Magnetic Technology—Fundamental Properties," IEEE Trans. Power Electron., vol. 29, no. 9, (2014).

[3] Christoph Marxgut, Jonas M'uhlethaler, Florian Krismer, and Johann W. Kolar, "Multiobjective Optimization of Ultraflat Magnetic Components With PCB-Integrated Core," IEEE Trans. Power Electron., vol. 28, no. 7, (2013).

[4] A. Ammouri, W. Ben Salah, S. Khachroumi, T. Ben Salah, F. Kourda, H. Morel, "Development of a physically-based planar inductors VHDL-AMS model for integrated power converter design," Eur. Phys. J. Appl. Phys. 66, 20901 (2014).

[5] Z. Ouyang, O. C. Thomsen and M. A. E. Andersen, "Optimal design and tradeoff analysis of planar transformer in high-power dc-dc converters," IEEE Trans. on Industrial Electronics, vol. 59, no. 7, pp. 2800 - 2810, (2012).

[6] Andersen, T.M.; Zingerli, C.M.; Krismer, F.; Kolar, J.W.; Ningning Wang; Mathuna, C.O., "Modeling and Pareto Optimization of Microfabricated Inductors for Power Supply on Chip," IEEE Trans. Power Electron., vol. 28, no. 9, (2013).

[7] J. M'uhlethaler, J. W. Kolar, and A. Ecklebe, "A Novel Approach for 3D Air Gap Reluctance Calculations," International Power Electronics Conference (ICPE- ASIA 2011).

[8] J. Romain Sibué, G. Kwimang, J. Paul Ferrieux, G. Meunier, J. Roudet, and R. Périot, "A Global Study of a Contactless Energy Transfer System: Analytical Design, Virtual Prototyping, and Experimental Validation," IEEE Trans. Power Electron., vol. 28, no. 10, (2013).

[9] A. D'Amico, C. Falconi, M. Bertsch, G. Ferri, R. Lojaco, M. Mazzotta, M. Santonico, G. Pennazza, "The Presence of the Fibonacci Numbers in Passive Ladder Networks: The Case of Forbidden Bands," IEEE Antennas and Propagation Magazine, vol. 56, no. 5, (2014).

[10] Salahuddin Raju, Rongxiang Wu, Mansun Chan, and C. Patrick Yue, "Modeling of Mutual Coupling Between Planar Inductors in Wireless Power Applications," IEEE Trans. Power Electron., vol. 29, no. 1, (2014).

[11] J. Ferreira, "Improved analytical modeling of conductive losses in magnetic components," IEEE Trans. Power Electron., vol. 9, no. 1, (1994).

[12] A. Ammouri, T. Ben Salah, F. Kourda, "Design and Modeling of Planar Magnetic Inductors for Power Converters Applications," 7th International Conference on Modelling, Identification and Control (ICMIC-2015).

[13] A. Ammouri, T. Ben Salah, F. Kourda, "Modeling and Simulation of a High-Frequency Planar Power Transformers," The 4th International Conference on Electrical Engineering (ICEE-2015).

[14] Fernando M. Janeiro, and Pedro M. Ramos, "Impedance Measurements Using Genetic Algorithms and Multiharmonic Signals," IEEE Trans. on Instrumentation and Measurement, vol. 58, no. 2, (2009).

[15] Masoud M. Shabestary, Ahmad Javid Ghanizadeh, G. B. Gharehpetian, and Mojtaba Agha-Mirsalim, "Ladder Network Parameters Determination Considering Nondominant Resonances of the Transformer Winding," IEEE Trans. on Power Delivery, vol. 29, no. 1, (2014).

[16] Peter Wallmeier, N. Frohliche, H. Grotstollen, "Automated optimization of high frequency inductors," IEEE (1998).

[17] Vytenis Leonavicius, Maeve Duffy, Ulrich Boeke, and Seán Cian Ó Mathúna Comparison of Realization Techniques for PFC Inductor Operating in Discontinuous Conduction Mode, "IEEE Trans. Power Electron., vol. 19, no. 2, (2004).